Applied Mathematical Sciences, Vol. 9, 2015, no. 110, 5451 - 5463
HIKARI Ltd, www.m-hikari.com
http://dx.doi.org/10.12988/ams.2015.56424

Mathematical Modelling and Experimental Assessment of Agrochemical Drift Using a Wind Tunnel

Dario Friso

Department of Land, Environment, Agriculture and Forestry - TESAF
Research Unit: Agricultural and Food Engineering
University of Padova, Viale dell'Università 16, Legnaro 35020, Padova, Italy

Cristiano Baldoin

Department of Land, Environment, Agriculture and Forestry - TESAF
Research Unit: Agricultural and Food Engineering
University of Padova, Viale dell'Università 16, Legnaro 35020, Padova, Italy

Abstract

With the aim to gain a better understanding of the phenomenon of drift occurring during spray application of agrochemicals to agricultural crops, a laboratory testing was carried out using a wind tunnel under controlled environmental conditions (wind, temperature and relative humidity RH). Spray drift was measured with wind velocity of 1, 3 and 5 m/s and RH of 30, 50 and 70%. Under medium to high wind velocities the effect of RH was negligible. These results suggested to work out a simplified mathematical modelling by assuming the absence of droplets evaporation by means of closed solutions of the equations of the droplets motion. The main result of the mathematical model is the removal of the droplets smaller than about 80 μm from the spray produced by the nozzles.

Keywords: Mathematical modelling, Droplet dynamics, Agrochemicals distribution, Drift, Crop protection, Environmental pollution, Wind tunnel, Agricultural engineering

1. Introduction

During the application of plant protection products to field crops, a fraction of spray droplets is normally dispersed in the environment because of weather events. This phenomenon is also known as drift and is mostly attributable to the wind, but also air humidity is responsible, to a smaller extent, since it increases evaporation when it is too low, thus causing a shrinking of the droplets and a greater fall out distance.
Since many years researchers have been working to reduce spray drift, for environmental and economic reasons [5, 10 and 14]. To this purpose, several field testing have been carried out, but not so many laboratory trials, under strictly controlled conditions, have been done.
Further, with reference to mathematical modelling, many studies were also made, but all of them laid to the numerical solution of the equation of the motion of droplets [1 and 2]. In last years, it was also proposed the mathematical modeling by computational fluid dynamics. This CFD methods [7, 8 and 11] are very good tools, but they need an high computing power and long calculation times. In addition, their use requires a qualified experience in the use of CFD (right choice of mesh, etc.).

The first aim of this work was the laboratory simulation of spray drift by means of a wind tunnel, fitted with a nozzle spraying water downwards; a series of trials were carried out under several wind velocities by weighing the amount of lost water. The measurements were replicated with three different conditions of air humidity.
The second goal was to find a closed solution to the differential equations, as made in previous researches [17 and 18], having the same objective in order to get a mathematical tool for the simulations [15].

2. Material and Methods

The purpose of the experimental research was the evaluation of the agrochemical drift without the influence of the variable climatic conditions that affect field tests. In order to run the experiment under standard conditions, a suitably equipped wind tunnel was built (fig. 1). The tunnel was 8 m long, with a square section of 0.8 x 0.8 m; the fan placed at one end was powered by a 3 kW tri-phase electric motor with adjustable air speed. The wind speed was measured at nozzle height using a digital anemometer that automatically calculated the average of the measured period, in this case, 30 seconds. The flat-fan nozzle (*Teejet* XRB 8002VS) with an 80° angle, anti-drip system and filter was placed at a height of 50 cm, 2.10 metres from the outlet and 4 metres from the fan, in order to regulate the air flow. It was supplied at bar 3.5 from a pressurised 25 dm^3 tank and an auxiliary pump for mixing; a digital manometer was installed close to the nozzle.

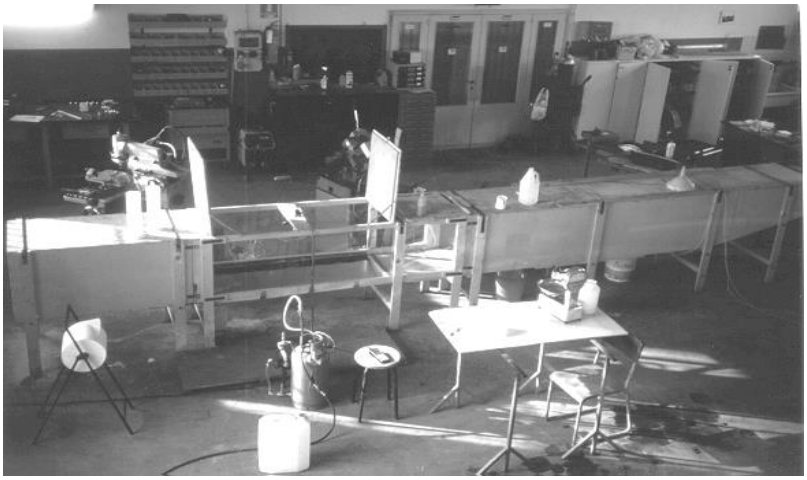

Fig. 1 – Overview of the wind tunnel.

In order to set up an environment large enough to operate under uniform temperature and humidity conditions, the tunnel has been mounted inside the laboratory (1,800 m^3 volume), where a 250,000 kJ air heating device and an humidifier allowed to set temperature and relative humidity.
The trials considered a quantitative measurement of the loss by drift was made through a series of sprayings in the tunnel, with subsequent precision weighing of the liquid collected in the planned interval of time (one minute). Each of these weighed amounts was subsequently related to the amount of liquid collected in the absence of wind; the drift has been computed by difference and expressed as a percentage as explained further.
The trials were carried out under a temperature of 27°C and under 3 levels of relative humidity (30, 50 and 70%). For each relative humidity, 4 wind velocities were tested (0, 1, 3 and 5 m/s). For each test three replications were made.

3. Results

As mentioned above, the trials were carried out under 3 conditions of relative humidity (30, 50 and 70%) with a mean temperature of 27°C; 4 wind velocities were tested (0, 1, 3 and 5 m/s), with three replications for each test. The percent loss by drift L for each replication was computed by weighing the liquid sprayed during 1 minute, and relating it to the amount collected without wind as follows:

$$L = \frac{m_o - m_n}{m_o} \cdot 100 \tag{1}$$

where: L is the amount of liquid lost (%); m_o is the mass of liquid (g) collected with wind speed = 0 m/s; m_n is the mass of liquid (g) collected with wind speed equal to n (m/s).

As shown in figure 2, with the highest values of wind velocity (5 m/s), average loss by drift is 15,8% with no significant differences related to relative humidity. At wind velocity of 3 m/s there are no significant differences on drift losses between relative humidity values of 50 and 70% with an average of 8%, while drift rises significantly to 10,1% with dry air (RH = 30%). Finally, loss by drift with wind velocity 1 m/s is obviously lower than with higher speed, and is also significantly affected by relative humidity.
With special reference to the highest wind velocities, pesticide losses by drift in the environment are not negligible and researchers are looking for possible solutions to the problem.

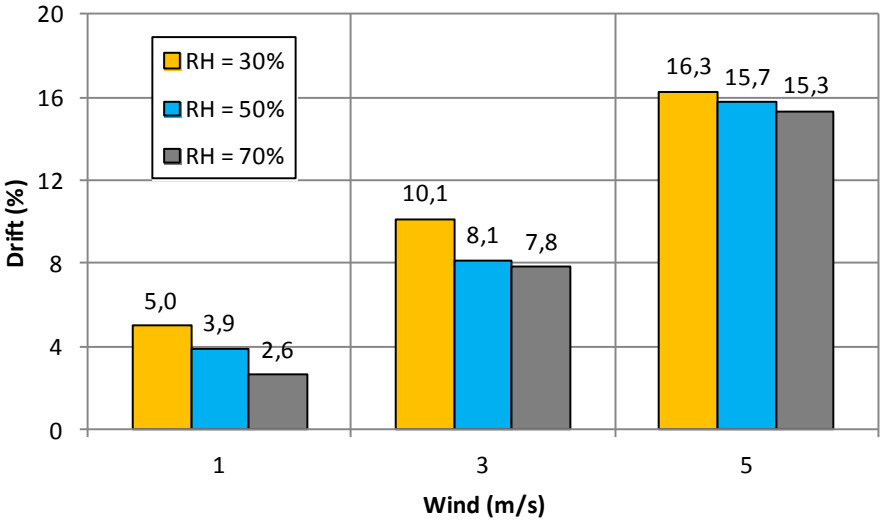

Fig. 2 – Loss by drift *L* (%) vs. wind velocity *w* (m/s) and relative humidity *RH* (%).

4. Mathematical modelling of droplet dynamic in wind tunnel

Droplets evaporation inside the tunnel was assumed as negligible as affecting drift. In fact, as shown in figure 2, with the exception of the lowest wind velocity *w*, loss by drift *L* (%) is not significantly affected by air humidity and, therefore, by droplets evaporation.
On the other hand, when wind velocity is lower (1 m/s), drift measured in the testing tunnel is anyway smaller, thus resulting a minor problem respect to the 2- and 3-fold values of L respectively with *w* of 3 e 5 m/s.
Coming back to the topic of pesticides application to agricultural crops, it should be pointed out that this operation is illegal in many countries during the central part of the day, when relative humidity is about 30%; instead, spray application must be operated earlier and later, when relative humidity rises over 50%.
The spectrum of the droplets emitted by the nozzles is characterized by a dimensional variability according to the well-known Rosin-Rammler size distribution [4 and 9].

The circumstance that, with low wind velocities (1 m/s) in the tunnel, influence of relative humidity arises is probably bound to the fact that under this condition only the smaller droplets are involved in drift. Further, Thompson and Ley [3] demonstrated that with evaporation $\frac{dD}{dt} \approx f\left(\frac{1}{D}\right)$, that is to say that the decrease rate of droplets diameter is inversely proportional to diameter itself. For example, 10-fold smaller droplets show an evaporation rate 10-fold greater [12 and 13]. So, drift is enhanced by the evaporation of these small droplets, which anyway represent a very small volume respect of the total one discharged by the nozzle (droplets with diameter less than 50 μm usually form less than 1% of the total volume produced by flat fan nozzles).

Therefore, going along with the simplifying assumption of neglecting droplets evaporation entails an error in forecasting drift in tunnel only in the case of low wind velocity.

Another assumption was made, related to accept the wind velocity as constant respect to the height. Under field conditions this assumption should not be accepted, since natural wind over the canopy appears as a gradient [3].

The last assumption regarded the droplets generation exactly on the nozzle orifice, while it is known that at this level a liquid sheet reaches out for some centimetres before breaking into ligaments: these are unstable and immediately afterwards break in turn, generating the droplets [6]. Therefore, droplets are actually generated some centimetres from the nozzle tip.

Now, the equation of the droplet motion in the tunnel is:

$$m \cdot \bar{a} = \Delta m \cdot \bar{g} - \bar{R} \tag{2}$$

where: m is the droplet mass; $\bar{a}$ is the acceleration; $\Delta m \cdot \bar{g}$ is weight after buoyancy; $\bar{R}$ is air resistance. Therefore (fig. 3) the equation (2) can be sketched out respect to vertical (y) and horizontal (x) directions, in order to understand their dynamic behaviour as affected by their diameter, resulting from side wind action:

$$m\frac{dv_y}{dt} = \Delta m \cdot g - R_y \tag{3}$$

$$m\frac{dv_x}{dt} = R_x \tag{4}$$

where: m is the droplet mass; $\Delta m \cdot g$ is weight after buoyancy; R_y is air resistance along y; R_x is air resistance along x; v_y and v_x are the components of the droplet velocity along y and x respectively; Assuming the droplet as spherical and developing, the following equations result:

$$\frac{dv_y}{dt} = \frac{\Delta\rho \cdot g}{\rho_l} - \frac{3}{4} C_d \frac{\rho_a}{\rho_l} \frac{u \cdot v_y}{D} \tag{5}$$

$$\frac{dv_x}{dt} = \frac{3}{4} C_d \frac{\rho_a}{\rho_l} \frac{u \cdot (w - v_x)}{D} \tag{6}$$

where: $\Delta\rho = \rho_l - \rho_a$; ρ_a is air density; ρ_l is the liquid density; D is the droplet diameter; u is the resultant speed responsible of the air resistance R. It is (fig 3): $u = \sqrt{v_y^2 + (w - v_x)^2}$, where w is the wind speed inside the tunnel. C_d is the drag coefficient; this last depends on the motion of the boundary layer:

$$C_d = \frac{24}{\mathrm{Re}} = \frac{24}{F \cdot u} \qquad \text{(laminar: } \mathrm{Re} \leq 2\text{)} \tag{7}$$

$$C_d = \frac{22}{\mathrm{Re}^{2/3}} = \frac{22}{F^{2/3} \cdot u^{2/3}} \qquad \text{(transitional: } 2 < \mathrm{Re} < 500\text{)} \tag{8}$$

where: Re is the Reynolds number, $\mathrm{Re} = \frac{\rho_a D}{\mu} u = F \cdot u$; $F = \frac{\rho_a D}{\mu}$; the case of turbulent motion was neglected, because it was considered only droplets having diameter D < 200 μm and initial velocity v_{yo} less than 20 m/s at the nozzle outlet, with liquid pressure < 4 bar and wind velocity w < 10 m/s, thus leading to Re < 500. The relation (8) come from the classical $C_d = 18{,}5 / \mathrm{Re}^{0,6}$ [6], adapted to have the exponent equal to 2/3 instead of 0.6, thus making easier getting the following closed solutions of the differential equations of motion.
Let's begin with the integration of motion equation along y, by inserting the relations (7) and (8) in the (5), thus obtaining respectively:

$$\frac{dv_y}{dt} = \frac{\Delta\rho \cdot g}{\rho_l} - \frac{18}{F \cdot D} \frac{\rho_a}{\rho_l} v_y = B - A \cdot v_y \tag{9}$$

$$\frac{dv_y}{dt} = \frac{\Delta\rho \cdot g}{\rho_l} - \frac{16{,}5}{F^{2/3} \cdot D} \frac{\rho_a}{\rho_l} u^{1/3} \cdot v_y = b - a \cdot u^{1/3} \cdot v_y \tag{10}$$

where the quantities A, B, a and b are defined as in (9) and (10). By a preliminary numerical integration of ODEs (4) and (5), the result $v_y / (w - v_x) \geq 5$, was obtained. This allows to write: $u = \sqrt{v_y^2 + (w - v_x)^2} \cong v_y$ with an error less than 3%. The differential equation (10) becomes:

$$\frac{dv_y}{dt} = b - a \cdot v_y^{4/3} \tag{11}$$

The (11) describes the initial motion of the droplet, under the effect of the high initial velocity v_{yo} produced by the pressure of the nozzle, with $Re_y > 2$. For large droplets (diameter > about 100 μm) the boundary layer motion remains transitional along the whole height h between the nozzle and the base of the tunnel (h = 0,5 m). When the droplet reaches the tunnel base, its velocity is specified with the symbol v_{yf}.

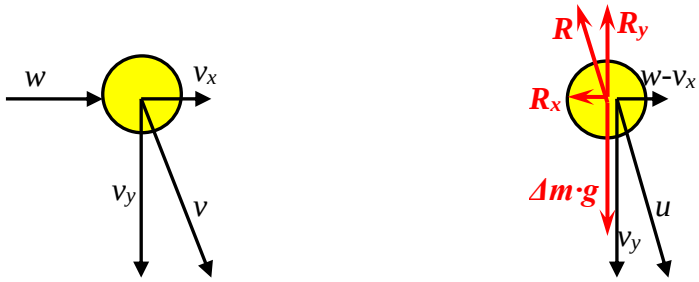

Fig. 3- Droplet velocity v and wind speed w (left). Forces acting on the droplet (right).

To determine whether the motion of the boundary layer remains transitional along the whole height h, it is necessary to compare the value of velocity v_{yf} to the one corresponding to $Re^* = 2$, namely to $v_{y^*} \cong u^* = Re^*/F = 2/F$. Since F depends on air viscosity and density and on the diameter D of the droplet, v_{y^*} depends on D too.
In order to find the final velocity it is necessary to rewrite equation (11) to relate v_y to the y coordinate, instead of the time t:

$$\frac{dv_y}{dt}\frac{dy}{dy} = b - a \cdot v_y^{4/3} \Rightarrow \frac{dv_y}{dy} = \frac{b}{v_y} - a \cdot v_y^{1/3} \tag{12}$$

By integrating the (12), under the initial condition $v_y = v_{yo}$ for $y = 0$, we get:

$$y = \frac{3b^{1/2}}{4a^{3/2}}\left[\ln\left(\frac{\left(a^{1/4}v_{yo}^{1/3} - b^{1/4}\right)\left(a^{1/4}v_{yo}^{1/3} + b^{1/4}\right)}{\left(a^{1/2}v_{yo}^{2/3} + b^{1/2}\right)}\right) - \ln\left(\frac{\left(a^{1/4}v_{y}^{1/3} - b^{1/4}\right)\left(a^{1/4}v_{y}^{1/3} + b^{1/4}\right)}{\left(a^{1/2}v_{y}^{2/3} + b^{1/2}\right)}\right)\right] + \frac{3}{2a}\left(v_{yo}^{2/3} - v_y^{2/3}\right) \tag{13}$$

If the (13) shows, with $v_y = v_{y^*}$ that $y \geq h$, than the motion of the boundary layer is transitional along the whole height h.
We go on by putting in the (13) $y = h$, then finding the numerical solution to $v_y = v_{yf}$. If the motion of the boundary layer remains transitional, finally we get $v_{yf} \geq v_{y^*}$ and the integration of (11) by separation of variables, under the initial

condition $v_y = v_{yo}$ with $t = 0$, allows to compute the total flight time t_t of the droplet, provided to put also $v_y = v_{yf}$ for $t = t_t$:

$$t_t = \frac{3}{4a^{3/4}b^{1/4}}\left[\ln\left(\frac{a^{1/4}v_{yo}^{1/3} - b^{1/4}}{a^{1/4}v_{yo}^{1/3} + b^{1/4}}\right) - \ln\left(\frac{a^{1/4}v_{yf}^{1/3} - b^{1/4}}{a^{1/4}v_{yf}^{1/3} + b^{1/4}}\right) + 2\arctan\left(\frac{a^{1/4}v_{yo}^{1/3}}{b^{1/4}}\right) - 2\arctan\left(\frac{a^{1/4}v_{yf}^{1/3}}{b^{1/4}}\right)\right] \tag{14}$$

If conversely the (13) shows, with $v_y = v_{y^*}$ that $y = y^* \le h$, than the motion of the boundary layer remains transitional only until the point y^*, while for the remainder of height $h - y^*$ the boundary layer becomes laminar.
What above mentioned occurs specially for very fine droplets, for which an initial step exists, as described by an equation similar to (14), but now giving the time of the first interval t^*:

$$t^* = \frac{3}{4a^{3/4}b^{1/4}}\left[\ln\left(\frac{a^{1/4}v_{yo}^{1/3} - b^{1/4}}{a^{1/4}v_{yo}^{1/3} + b^{1/4}}\right) - \ln\left(\frac{a^{1/4}v_{y^*}^{1/3} - b^{1/4}}{a^{1/4}v_{y^*}^{1/3} + b^{1/4}}\right) + 2\arctan\left(\frac{a^{1/4}v_{yo}^{1/3}}{b^{1/4}}\right) - 2\arctan\left(\frac{a^{1/4}v_{y^*}^{1/3}}{b^{1/4}}\right)\right] \tag{15}$$

The second step of the motion is described by the differential equation (10), which is linear and its integration by separation of variables returns:

$$v_y = \frac{B}{A} + \left(v_{y^*} - \frac{B}{A}\right)\cdot e^{-A\cdot t} \tag{16}$$

where: t is the time, considered as null at the beginning of the second interval of the motion; B/A coincides with Stokes sedimentation velocity [6]; the (16) was obtained under the initial condition $v_y = v_{y^*}$ for $t = 0$, where v_{y^*} is the velocity corresponding to $\mathrm{Re}^* = 2$. Therefore, its value is: $v_{y^*} \cong u^* = \mathrm{Re}^*/F = 2/F$; where F is: $F = \frac{\rho_a D}{\mu}$.
By integrating beyond the (16) between initial (y^*) and final (h) height, respectively with the initial time of the second interval $t = 0$ and the final time $t = t_2$ corresponding to the impact with the base of the tunnel, we get:

$$h - y^* = \frac{B}{A}t_2 + \frac{1}{A}\left(v_{y^*} - \frac{B}{A}\right)\left(1 - e^{-A\cdot t_2}\right) \tag{17}$$

The (17) allows to calculate the duration t_2 of the second interval (laminar boundary layer). Therefore, by adding t_2 to the time of the first interval t^*, the total flight time t_t results: $t_t = t^* + t_2$.

Let's move to the integration of the equation of the motion along *x*, by putting the (7) and (8) into the (6) and thus getting respectively:

$$\frac{dv_x}{dt} = \frac{18}{F \cdot D}\frac{\rho_a}{\rho_l}\left(w - v_x\right) = A \cdot \left(w - v_x\right) \tag{18}$$

$$\frac{dv_x}{dt} = \frac{16.5}{F^{2/3} \cdot D}\frac{\rho_a}{\rho_l}u^{1/3} \cdot \left(w - v_x\right) = a \cdot u^{1/3} \cdot \left(w - v_x\right) \tag{19}$$

where the symbols *A* and *a* group some quantities in the (18) and respectively in the (19), and coincide with the symbols *A* and *a* used in (9) and (10).
Now, with a negligible error on the subsequent calculation of the drift, the assumption: $u^{1/3} \approx v_{ym}^{1/3} = \frac{v_{y0}^{1/3} + v_{yf}^{1/3}}{2}$, where v_{ym} is the mean speed along y-axis during first time interval 0-t^*, was made. Therefore the (19) becomes:

$$\frac{dv_x}{dt} = a \cdot v_{ym}^{1/3} \cdot \left(w - v_x\right) \tag{20}$$

Summarizing, the ODE (20) describes the motion of the droplet when the motion in boundary layer is transitional (Re > 2) and this may occur during the first time interval 0-t^*. The integration of the (20) by separation of variables returns the terminal velocity at the time t^*:

$$v_{x^*} = w \cdot \left(1 - e^{-a \cdot v_{ym}^{1/3} \cdot t^*}\right) \tag{21}$$

By integrating beyond the (21) we get the horizontal distance x^* travelled by the droplet during the first period 0-t^*:

$$x^* = w \cdot t^* - \frac{w}{a \cdot v_{ym}^{1/3}}\left(1 - e^{-a \cdot v_{ym}^{1/3} \cdot t^*}\right) \tag{22}$$

When the time t^* is passed, the second period begins with the laminar motion of the boundary layer. This period lasts a time t_2 calculated by the (17) and, hence, is the total vertical flight time, net of the time t^* resulting from (15):

$$t_2 = t_t - t^* \tag{23}$$

The differential equation (18) is now valid; its integration produces:

$$v_x = w - \left(w - v_{x^*}\right) \cdot e^{-A \cdot t} \tag{24}$$

where: *t* is the time, assumed as null at the beginning of this second part of the

motion along x (second period); the (24) was obtained assuming the initial condition $v_x = v_{x^*}$ for $t = 0$, with v_{x^*} obtained by the (21). The further integration of the (24) returns the distance x_2 travelled during the second period for $\mathrm{Re} \leq 2$, which lasts as according to (17) at a time t_2:

$$x_2 = w \cdot t_2 - \frac{(w - v_{x^*})}{A} \cdot \left(1 - e^{-A \cdot t_2}\right) \tag{25}$$

The total distance travelled, defined as drift, therefore results:

$$x_t = x^* + x_2 \tag{26}$$

When droplets diameters is greater than about 200 μm, the time t^*, deduced from the (15) and corresponding to the reaching of the critical condition $\mathrm{Re}^* = 2$, results greater than the total flight time t_t. In this case, the second period of the laminar motion of the boundary layer will be absent and, therefore, the value of drift results from an equation similar to the (22):

$$x_t = w \cdot t_t - \frac{w}{a \cdot v_{ym}^{1/3}} \left(1 - e^{-a \cdot v_{ym}^{1/3} \cdot t_t}\right) \tag{27}$$

Figure 4 shows the drift simulation as resulting from the application of the equations (22), (25) and (26); drift x_t is function of droplets diameter and wind velocity w. As the graphs point out, a 90 μm diameter droplet shows a drift x_t not exceeding 10 m when w = 1÷7 m/s, while a 30 μm particle reveals a drift of 50 m when w = 3 m/s and 90 m when w = 5 m/s.
Finally, according to the present modelling, a 10 μm droplet travels 1 km when w = 7 m/s. Actually, the forecast is underestimated, because evaporation causes a fast decay of droplets diameter during the flight.

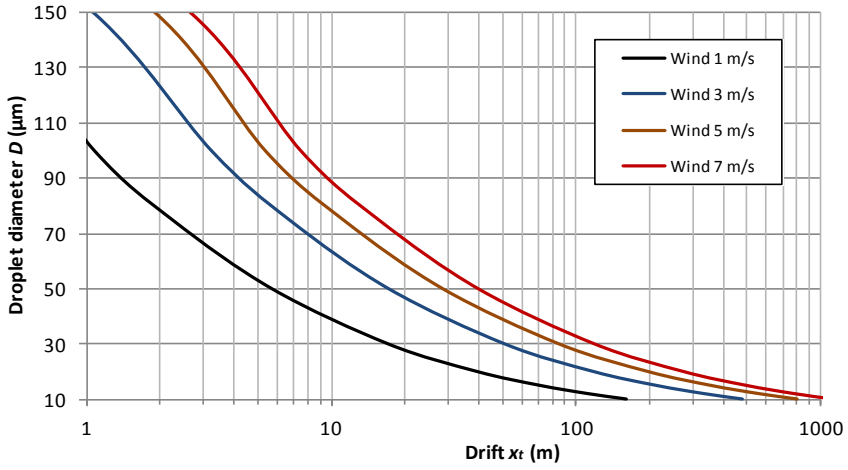

Fig. 4 – Drift vs. droplet diameter and wind velocity.

5. Conclusion

Experimental testing to assess loss by drift was carried out in an indoor laboratory to control air relative humidity, and using a wind tunnel to get a uniform air velocity; these climate conditions are not controllable in an open field testing.
The results show that only under low wind velocity air humidity affects losses by drift. This occurs because evaporation, when air humidity is low, causes a fast decay of the diameter of the finest droplets, which are the only one involved in drift when wind is low. When wind velocity is medium to high, the effect of humidity, and therefore of evaporation, becomes negligible because in this case the huge loss by drift is due to larger droplets which, because of their lower surface to volume ratio, show a very smaller decay of diameter.
The above results suggested to work out a mathematical modelling, simplified by the absence of evaporation, obtained with closed solutions of the differential equations of the motion of droplets.
Consequently, the proposed mathematical modelling arises as a closed solution of the particle dynamics equations as an alternative to numerical integrations, which don't easily return an immediate simulation.
Mathematical modelling suggested, as the main result, to remove – or at least reduce – from the droplet spectrum produced by the nozzles the fraction of particles smaller than 80÷90 μm.
A feasible way to get this goal, to be verified in wind tunnel, is the modification of the rheological properties of liquid used to dilute agrochemicals by adding some chemical thickeners, by increasing of viscosity [16].
Finally, it should be useful to improve the mathematical model to manage to predict not only drift distance of the droplets, but also the amount of loss by drift, in order to use it as a support tool to forecast the same losses during on field agrochemical distribution.

References

[1] C.E. Goering, L.E. Bode, M.R. Gebhardt, Mathematical model of spray droplet deceleration and evaporation, *Transactions of the ASAE*, **15** (1972), 220 - 225. http://dx.doi.org/10.13031/2013.37871

[2] E. Threadgill and D. Smith, Effects of physical and meteorological parameters on the drift of controlled-size droplets, *Transactions of the ASAE*, **18** (1975), 51 - 56. http://dx.doi.org/10.13031/2013.36523

[3] N. Thompson, A. Ley, Estimating spray drift using a random-walk model of evaporating drops, *Journal of Agricultural Engineering Research*, **28** (1983), 419 - 435. http://dx.doi.org/10.1016/0021-8634(83)90134-8

[4] A.G. Bailey, W. Balachandran and T.J. Williams, The rosin-rammler size distribution for liquid droplet ensembles, *Journal of Aerosol Sciences*, **14** (1983), no. 1, 39 - 46. http://dx.doi.org/10.1016/0021-8502(83)90083-6

[5] Y. Gil and C. Sinfort, Emission of pesticides to the air during sprayer application: A bibliographic review, *Atmospheric Environment*, **39** (2005), 5183 - 5193. http://dx.doi.org/10.1016/j.atmosenv.2005.05.019

[6] R. Perry and D. Green, *Perry's Chemical Engineering's Handbook*, McGraw-Hill, New York, 2007.

[7] K. Baetens, D. Nuyttens, P. Verboven, M. De Schampheleire, B. Nicolaï, H. Ramon, Predicting drift from field spraying by means of a 3D computational fluid dynamics model, *Computers and Electronics in Agriculture*, **56** (2007), no. 2, 161 - 173. http://dx.doi.org/10.1016/j.compag.2007.01.009

[8] D. Nuyttens, M.D. Schampheleire, K. Baetens, E. Brusselman, D. Dekeyser, P. Verboven, Drift from field crop sprayers using an integrated approach: Results of a five-year study, *Transactions of the ASABE*, 54 (2011), no. 2, 403 - 408. http://dx.doi.org/10.13031/2013.36442

[9] F. Agüera, D. Nuyttens, F. Carvajal, J. Sánchez-Hermosilla, Fractal analysis of agricultural nozzles spray, *Scientia Agricola*, **69** (2012), no. 1, 6 - 12.

[10] D. Falchieri, New application method for reducing pesticide rate/ha and cost in plant protection, *Outlooks on Pest Management*, **24** (2013), no. 6, 257 - 261. http://dx.doi.org/10.1564/v24_dec_05

[11] J. Yuan, X. Liu, X. Zhang, W. Zuo, X. Wang, L. Chen, Modeling and compensation for characteristic of droplet drift on air-assisted boom spraying accounting for wind speeds, *Nongye Gongcheng Xuebao/Transactions of the Chinese Society of Agricultural Engineering*, **29** (2013), no. 14-15 July, 45 - 52.

[12] M. Bietresato, D. Friso, Durability Test on an Agricultural Tractor Engine Fuelled with Pure Biodiesel (B100), *Turkish Journal of Agriculture and Forestry*, **38** (2014), np. 2, 214 - 223. http://dx.doi.org/10.3906/tar-1302-51

[13] D. Friso, Brake Thermal Efficiency and BSFC of Diesel Engines: Mathematical Modeling and Comparison Between Diesel Oil and Biodiesel Fueling, *Applied Mathematical Sciences*, **8** (2014), no. 130, 6515 - 6528. http://dx.doi.org/10.12988/ams.2014.46444

[14] G. Doruchowski, P. Balsari, P. Marucco, A. Herbst, H.J. Wehmann, M. Roettele, E. Gil, S. Codis, E. Pauwelyn, Decision support tools for environ-

mentally safe use of pesticides, *Communications in agricultural and applied biological sciences*, **78** (2013), no. 2, 37 - 45.

[15] D. Friso, Energy Saving with Total Energy System for Cold Storage in Italy: Mathematical Modeling and Simulation, Exergetic and Economic Analysis, *Applied Mathematical Sciences*, **8** (2014), no. 130, 6529 - 6546. http://dx.doi.org/10.12988/ams.2014.46443

[16] S. Choi, Y. Oh, The Various Analysis on Characteristics of BD from Animal Fats. *Contemporary Engineering Sciences*, **7** (2014), no. 22, 1163 - 1170. http://dx.doi.org/10.12988/ces.2014.49145

[17] D. Friso, C. Baldoin, F. Pezzi, Mathematical Modeling of the Dynamics of Air Jet Crossing the Canopy of Tree Crops during Pesticide Application, *Applied Mathematical Sciences*, **9** (2015), no. 26, 1281 - 1296. http://dx.doi.org/10.12988/ams.2015.5145

[18] D. Friso, A Mathematical Solution for Food Thermal Process Design, *Applied Mathematical Sciences*, **9** (2015), no. 6, 255 - 270. http://dx.doi.org/10.12988/ams.2015.411980

Received: June 24, 2015; Published: August 25, 2015